A&A 481, 239–246 (2008)
DOI: 10.1051/0004-6361:20078689

Astronomy & Astrophysics

Kink oscillations in magnetic tubes with twisted annulus

B. K. Carter and R. Erdélyi

Solar Physics & Space Plasma Research Centre (SP^{2}RC), Dept. of Applied Mathematics, The University of Sheffield, Hicks Building, Hounsfield Road, Sheffield, S3 7RH, UK
e-mail: [robertus;b.carter]@sheffield.ac.uk

Received 17 September 2007 / Accepted 14 January 2008

ABSTRACT

Aims. We study kink waves in a magnetic flux tube modelled as a straight core surrounded by a magnetically twisted annulus, both embedded in a straight ambient external field, and derive the dispersion relation for this configuration.
Methods. The existence and behaviour of the kink modes are examined with specific attention to the effect that the addition of magnetic twist has on phase speeds and periods. Analytic expansions to the short and long wavelength approximations are also considered.
Results. The magnetic twist is found to introduce of an infinite set of body modes into solutions of the dispersion relation not present in the untwisted case. Moreover, for the kink modes, the width of interval of this infinite set, generally found to occupy phase speeds around the annulus' longitudinal Alfvén speed, increases for longer wavelengths. Two surface modes are also present in the solution, one at each surface: the internal and the external edges of the annulus. The magnetic twist is found to increase or decrease the phase speeds of these surface modes that are depending on the ratio of internal and external Alfvén speeds in the flux tube.
Conclusions. The magnetic twist of the annulus region of a flux tube is found to have a marked effect on the phase speeds of occurring modes. A straight annulus layer increased (or decreased) the periods of the surface modes for a tube modelled as a density (magnetic) enhancement. The addition of twist reduces the periods of the modes in both cases.

Key words. magnetohydrodynamics (MHD) – waves – Sun: oscillations – Sun: magnetic fields

1. Introduction

Oscillations of magnetic tubes in the form of a magnetic core and shell have been investigated in detail by, amongst others, Carter & Erdélyi (2004, 2007), Mikhalyaev & Solov'ev (2004, 2005), and Erdélyi & Carter (2006). These works extended the much studied model of a single straight magnetic tube embedded in a straight external magnetic field put forward by Edwin & Roberts (1983) to a co-axial double flux tube consisting of a core and shell region each with distinct magnetic field. In the single tube case, for a slender flux tube, one may define two characteristic speeds of propagation. These are the subsonic, sub-Alfvénic tube speed $c_{\rm T}$ given by

$$c_{\rm T} = \frac{c_0 v_{\rm A}}{(c_0^2 + v_{\rm A}^2)^{1/2}},$$

for sound speed c_0 and Alfvén speed $v_{\rm A}$ and the kink speed, $c_{\rm k}$, given by

$$c_{\rm k}^2 = \frac{\rho_0 v_{\rm A}^2 + \rho_e v_{\rm Ae}^2}{\rho_0 + \rho_{\rm e}},$$

in which the densities and Alfvén speeds inside and outside the tube are ρ_0, $v_{\rm A}$, $\rho_{\rm e}$ and $v_{\rm Ae}$, respectively. Note here that the kink speed, $c_{\rm k}$, is independent of the sound speed (and hence compressibility). In the limit of incompressibility this speed plays further roles for MHD waves in a magnetised plasma. E.g. it is the phase speed of a long wavelength kink disturbance or is the common speed of both the sausage and kink modes in the short wavelength (wide cylinder) limit of oscillating magnetic flux tubes.

For the core-shell type flux tube model without a magnetic twist, Mikhalyaev & Solov'ev (2005, hereafter MS05) and Carter & Erdélyi (2007) found that there are twice as many surface modes as for the single tube case and moreover that the modes have different properties. MS05 showed the slow modes in the thin tube occur for all azimuthal wave numbers m while the fast modes exist only for $m > 0$. For coronal conditions, i.e. $v_{\rm A} \gg c_{\rm s}$, the two slow modes are trapped in the tube – one by the core, the other by the shell. The fast modes are also trapped by the core and the shell provided the shell Alfvén speed lies between the Alfvén speeds in the core and external regions, e.g. $v_{\rm Ai} < v_{\rm A0} < v_{\rm Ae}$. (In this paper we shall use the subscripts i, 0 and e to denote quantities corresponding to the core, shell and external regions, respectively).

Carter & Erdélyi (2007) investigate, for the incompressible non-twisted case, the effect of the shell width on the periods of propagating waves for both the sausage and kink modes of oscillation. They find that for typical photospheric parameters ($v_{\rm Ai} > v_{\rm A0} \gg v_{\rm Ae}$) the periods of the modes are decreased by the existence of an annulus layer whereas periods are increased in the case of a dense tube ($v_{\rm Ai} < v_{\rm A0} < v_{\rm Ae}$).

A natural extension of these previous works is that of the addition of magnetic twist. A uniformly twisted magnetic tube embedded in a straight magnetic environment was studied for an incompressible plasma by Bennett et al. (1999); Erdélyi & Fedun (2006, 2007). Some new features arising due to the introduction of twist were found. Most prominent was the existence of an infinite set of body modes which is absent in the incompressible straight field case and is centered around the internal Alfvén speed, $v_{\rm Ai}$, for the sausage modes and in shorter wavelengths for the kink modes. Another aspect was the coupling of the

degenerated magneto-acoustic mode to the Alfvén mode even in linear theory of the incompressible limit.

Erdélyi & Carter (2006) further extended the studies of MHD waves in a twisted flux tube by considering a magnetically twisted shell geometry. Specific modes of propagation and associated phase speeds were studied for a magnetic configuration in which a uniform twist is applied to the shell region. Only the more tractable sausage modes were considered. By introducing a magnetic twist to the shell it was found that, where there were only surface modes before, there now existed an infinite set of body modes which increased in width as the strength of the twist was increased. It was also found that the phase speeds of the surface modes were changed significantly (up to 5%) by increasing the twist just a small amount.

In this paper, intended as a natural extension to Erdélyi & Carter (2006), we analyse a similar magnetic shell structure for the kink modes, with specific attention given to the modes of oscillation present and to the effect of the applied twist on wave periods of kink oscillations.

We investigate kink mode propagation in a magnetic tube consisting of a straight magnetic core and twisted magnetic annulus, or shell, embedded in a straight magnetic ambient external environment. We apply the general dispersion relation, as found by Erdélyi & Carter (2006), to two applicable situations in the solar atmosphere: (i) to a tube as a magnetic enhancement with a weak magnetic environment and (ii) to a tube defined by a density enhancement. For further insight into behaviour of the kink modes, long and short wavelength approximations are considered.

Since the kink modes, in general, are highly incompressible the limit of incompressibility is of great interest, not just for wave studies in the deeper part of the solar atmosphere (e.g. where the plasma-beta is high) but can also be directly applicable from the lower solar atmosphere to the corona.

For observational motivation supporting the study of MHD wave oscillations in magnetic waveguides see, for example, reviews by Aschwanden (2004), Banerjee et al. (2007), Nakariakov & Verwichte (2005). These reviews give insight into the current state-of-the-art of solar magneto-seismology, a rapidly emerging field of solar physics, with several more references to specific MHD waves and oscillations observed in the magnetised and highly structured solar atmosphere. As a specific example, Kukhianidze et al. (2006), Zaqarashvili et al. (2007) recently discovered Doppler oscillations in spicules in the lower atmosphere with estimated periods ranging between 20 and 110 s. They attributed these motions to kink waves in a region in which motions are approximated by incompressibility.

It is useful to note here that by Fourier analysing the linear MHD equations like $e^{im\theta}$ and by taking $m = 1$ (kink modes only) we are considering a non-axisymmetric mode of oscillation. The torsional Alfvén mode, being axisymmetric, is now removed from the system and hence will not interact with modes present in the analysis of this paper (see e.g. Erdélyi & Fedun 2007).

2. The magnetic annulus

2.1. The dispersion relation

We restrict our investigation to an incompressible plasma for which the fast waves are removed from the system and we also lose phase speed distinction between the Alfvén and slow modes, the modes being distinguishable by direction of propagation only. A magnetic flux tube is modelled as a magnetically twisted annulus (or shell) layer surrounding a straight magnetic core all embedded in a straight magnetic ambient environment as shown in Fig. 1. This equilibrium configuration was investigated previously by Erdélyi & Carter (2006) and can be given by

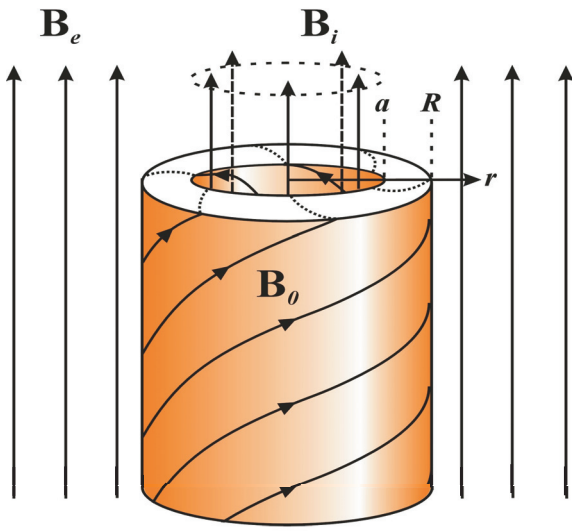

Fig. 1. Configuration of the magnetic tube consisting of a twisted magnetic annulus and straight core embedded in an ambient straight external magnetic field.

$$\boldsymbol{B} = \begin{cases} \boldsymbol{B}_{\rm i} = (0, 0, B_{\rm i}), & r < a, \\ \boldsymbol{B}_0 = (0, A_0 r, B_0), & a < r < R, \\ \boldsymbol{B}_{\rm e} = (0, 0, B_{\rm e}), & r > R, \end{cases} \tag{1}$$

with equilibrium pressure $p_0(r)$ taken to be

$$p_0(r) = \begin{cases} p_{\rm i}, & r < a, \\ p_0(a) - \frac{A_0^2 r^2}{\mu}, & a < r < R, \\ p_{\rm e}, & r > R, \end{cases} \tag{2}$$

where $p_{\rm i}$ and $p_{\rm e}$ are the uniform plasma pressures in the untwisted internal and external regions and $p_0(a)$ is the plasma pressure at the inner boundary of the twisted annulus layer. The pressure perturbation is found to be

$$p_{\rm T} = \alpha I_1(k_z r), \tag{3}$$

for the core region ($r < a$),

$$p_{\rm T} = \delta K_1(k_z r), \tag{4}$$

for in the environment ($r > R$) and

$$p_{\rm T} = \begin{cases} \beta I_1(m_0 r) + \gamma K_1(m_0 r) & m_0^2 & > 0, \\ \beta J_1(n_0 r) + \gamma Y_1(n_0 r) & n_0^2 = -m_0^2 & > 0, \end{cases} \tag{5}$$

in the twisted annulus ($a < r < R$) where α, β, γ and δ are arbitrary constants determined by the boundary conditions. The general dispersion relation can then be found for a magnetic flux tube with a straight magnetic core and uniform magnetic twist in the annulus region to take the following form:

$$\frac{\Xi_{aK} - \Xi_{\rm i} + \Xi_{aK}\Xi_{\rm i}\frac{A_0^2}{\mu}}{\Xi_{aI} - \Xi_{\rm i} + \Xi_{aI}\Xi_{\rm i}\frac{A_0^2}{\mu}} \frac{K_m(m_0 a)}{I_m(m_0 a)} = \frac{K_m(m_0 R)}{I_m(m_0 R)} \frac{\Xi_{RK} - \Xi_{\rm e} + \Xi_{RK}\Xi_{\rm e}\frac{A_0^2}{\mu}}{\Xi_{RI} - \Xi_{\rm e} + \Xi_{RI}\Xi_{\rm e}\frac{A_0^2}{\mu}}, \quad m_0^2 > 0, \tag{6a}$$

for purely surface waves, and

$$\frac{\Xi_{aY} - \Xi_{\rm i} + \Xi_{aY}\Xi_{\rm i}\frac{A_0^2}{\mu}}{\Xi_{aJ} - \Xi_{\rm i} + \Xi_{aJ}\Xi_{\rm i}\frac{A_0^2}{\mu}}\frac{Y_m(n_0 a)}{J_m(n_0 a)} =$$

$$\frac{Y_m(n_0 R)}{J_m(n_0 R)}\frac{\Xi_{RY} - \Xi_{\rm e} + \Xi_{RY}\Xi_{\rm e}\frac{A_0^2}{\mu}}{\Xi_{RJ} - \Xi_{\rm e} + \Xi_{RJ}\Xi_{\rm e}\frac{A_0^2}{\mu}}, \quad m_0^2 < 0, \tag{6b}$$

for body waves. Here

$$\Xi_{\alpha X} = \frac{(\omega^2 - \omega_{\rm A0}^2)\frac{m_0\alpha X_m'(m_0\alpha)}{X_m(m_0\alpha)} - \frac{2mA_0\omega_{\rm A0}}{\sqrt{\mu\rho_0}}}{\rho_0(\omega^2 - \omega_{\rm A0}^2)^2 - \frac{4A_0^2\omega_{\rm A0}^2}{\mu}},$$

where the dash $'$ denotes the derivative with respect to the argument of the Bessel functions, X denotes the corresponding Bessel function J, Y or modified Bessel function I, K, and α is replaced by a, R for the corresponding internal or external boundary of the annulus. Further,

$$\begin{aligned}
\Xi_{\rm i} &= \frac{|k|aI_m'(|k|a)}{\rho_{\rm i}(\omega^2 - \omega_{\rm Ai}^2)I_m(|k|a)},\\
\Xi_{\rm e} &= \frac{|k|RK_m'(|k|R)}{\rho_{\rm e}(\omega^2 - \omega_{\rm Ae}^2)K_m(|k|R)},\\
m_0^2 &= k_z^2\left(1 - \frac{4A_0^2\omega_{\rm A0}^2}{\mu\rho_0(\omega^2 - \omega_{\rm A0}^2)^2}\right) = -n_0^2.
\end{aligned} \tag{7}$$

The Alfvén frequencies in the annulus, internal and external regions are given by $\omega_{\rm A0}$, $\omega_{\rm Ai}$, and $\omega_{\rm Ae}$, respectively such that

$$\begin{aligned}
\omega_{\rm A0} &= \frac{1}{\sqrt{\mu\rho_0}}(mA_0 + k_z B_0),\\
\omega_{\rm Ai} &= \frac{k_z B_{\rm i}}{\sqrt{\mu\rho_{\rm i}}}, \quad \omega_{\rm Ae} = \frac{k_z B_{\rm e}}{\sqrt{\mu\rho_{\rm e}}}.
\end{aligned}$$

A_0 measures the strength of the uniform magnetic twist in the annulus region. Erdélyi & Carter (2006) investigated this dispersion relation for sausage modes only, i.e. in the case when $m = 0$. Here we embark to analyse the mathematically perhaps more complicated $m = 1$ kink modes.

3. Analysis and results

Two specific examples, distinct through the ratios of Alfvén speeds in each region, are used for the analysis of the general dispersion relation Eqs. (6a,b): $v_{\rm Ai} > v_{\rm A0} \gg v_{\rm Ae}$ and $v_{\rm Ai} < v_{\rm A0} < v_{\rm Ae}$. In the analysis that follows the value of the twist $B_\theta(r)/B_z$ is taken at the internal core-annulus boundary $r = a$.

3.1. Magnetically enhanced tubes

Let us assume that the tube is distinct to its environment due to a magnetic enhancement and that it has otherwise uniform density throughout ($B_{\rm i} > B_0 \gg B_{\rm e}$, $\rho_{\rm i} = \rho_0 = \rho_{\rm e}$) so that the Alfvén speeds for each region satisfy the rendering $v_{\rm Ai} > v_{\rm A0} \gg v_{\rm Ae}$. These conditions may be applicable to subsurface or lower solar atmosphere up to the chromosphere and, since we consider kink modes only, incompressibility will, of course, less restrict a wider direct application even in the higher solar atmosphere. Further, we shall consider only weak twists i.e. $B_\theta/B_z < 1$.

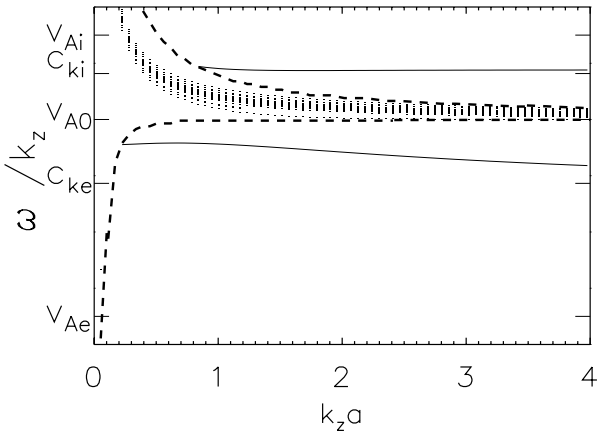

Fig. 2. Plot of solutions to Eqs. (6a,b) for typical photospheric parameters ($v_{\rm Ai} > v_{\rm A0} \gg v_{\rm Ae}$) for a magnetic twist ($B_\theta/B_z$) of 0.1 and relative core width $a/R = 0.8$. Shown are the infinite set of body (dotted) modes, two surface (solid) modes and the dashed envelope separating the modes given by $m_0^2 \equiv 0$.

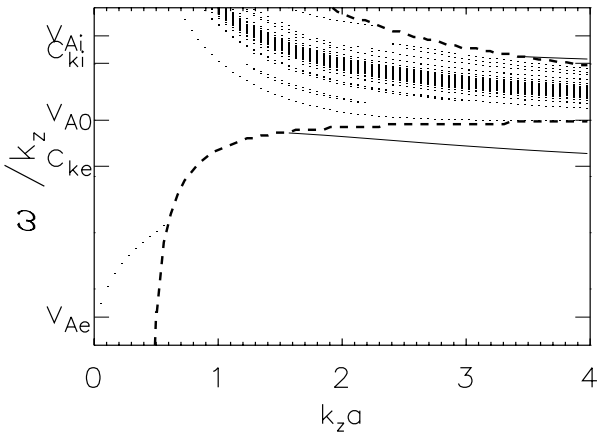

Fig. 3. Same as Fig. 2 but for a magnetic twist of 0.5.

Figures 2 and 3 show, for a twist, B_θ/B_z, of 0.1 and 0.5, the dispersion curves for Eqs. (6a,b) for the $m = 1$ (kink) modes for a fixed annulus width (the emphasis here is on the effect of the applied magnetic twist) so that $a/R = 0.8$. As in the case of sausage waves (Erdélyi & Carter 2006), there exists an infinite set of body modes that broadens as twist is increased. The envelope separating body and surface modes ($m_0^2 \equiv 0$, indicated by the dashed lines) is not, anymore, symmetrical about $v_{\rm A0}$ but stretches to larger phase speeds as $k_z a$ decreases. The set of body modes follows this trend; the phase speeds of modes becoming increasingly larger as wavelength increases indicating strong dispersion. The two surface modes, given by the solid curves in Figs. 2 and 3, are trapped, as in the untwisted case (MS05; Carter & Erdélyi 2007), one by the core, the other by the annulus, and they propagate with phase speeds in the proximity of $c_{\rm ki}$ and $c_{\rm ke}$, respectively, the latter showing somewhat more dispersion. For larger twists, the separating envelope (the dashed curves separating the region where body modes exist and the region where we find surface modes only) expands meaning that the surface waves are only solutions for shorter wavelengths. The surface modes do not appear to change behaviour into body modes directly across the $m_0 = 0$ separating envelope as with the single twisted tube (as in Bennett et al. 1999) and so it would seem that

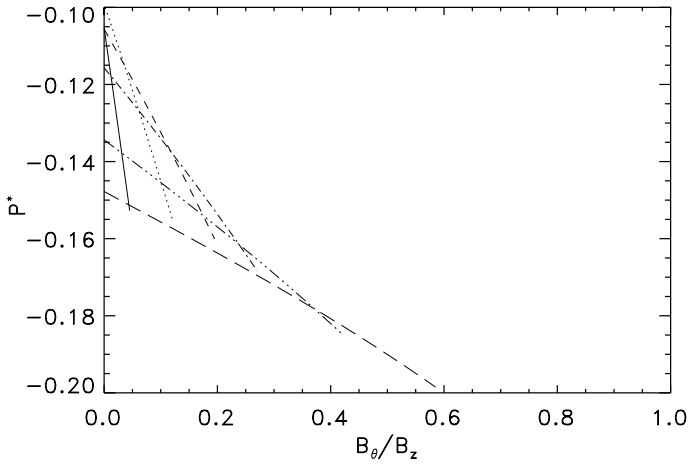

Fig. 4. Plot, for photospheric parameters, of the relative difference, P^*, between the period, P, of the surface mode with phase speed approximately $c_{\rm ki}$ and the period, $P_{\rm ER}$, of the straight, single monolithic tube with internal Alfvén speed equal to the core Alfvén speed, $v_{\rm Ai}$, in the core-shell model ($P^* := (P - P_{\rm ER})/P_{\rm ER}$). Shown are lines for $k_z a = 0.5$ (solid), 1 (dot), 1.5 (dash), 2 (dot-dash), 3 (3dot-dash) and 4 (long dash). $a/R = 0.8$.

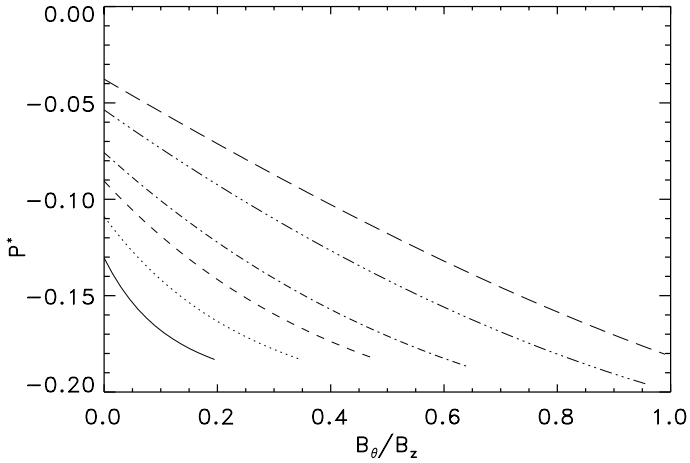

Fig. 5. Same as Fig. 4 but for the core-shell model surface mode with phase speed approximately $c_{\rm ke}$ for a single tube internal Alfvén speed equal to the shell Alfvén speed, $v_{\rm A0}$.

the twisted annulus configuration acts to cause a "splitting" of the hybrid modes.

Let us now investigate the effect of a twisted annulus on wave periods. Figures 4 and 5 show the relative changes in surface mode periods compared to an incompressible straight magnetic monolithic tube (as in Edwin & Roberts 1983) for different degrees of twist. In plots throughout the paper we use the relative period difference, P^*, between the period, P, of the surface mode in question and the period, $P_{\rm ER}$, of the straight, single monolithic tube with a certain given internal Alfvén speed where $P^* = (P - P_{\rm ER})/P_{\rm ER}$.

Figure 4 shows the relative difference, P^*, between the period, P, of the surface mode at $r = a$ shown in Figs. 2 and 3 as the upper of the two surface modes and the period, $P_{\rm ER}$, of the straight, single monolithic tube with internal Alfvén speed taken as equal to the core Alfvén speed, $v_{\rm Ai}$, in the core-shell model. The introduction of a straight annulus layer originally decreased the periods of the mode and it is found that the application of twist to the configuration further reduces these periods. The percentage change in phase speed due to the twist from the

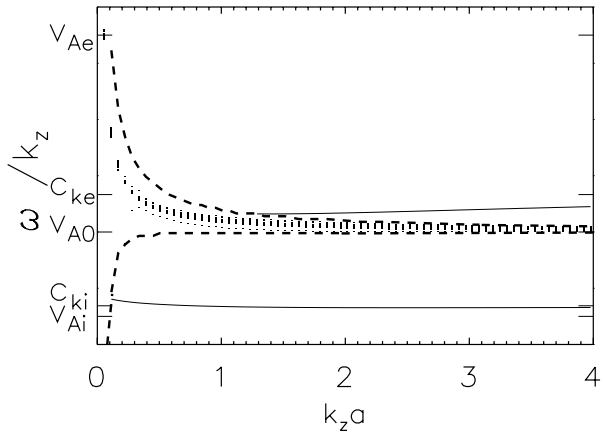

Fig. 6. Plot of the solution to the dispersion relation Eqs. (6a,b) for parameters approximating a dense tube ($v_{\rm Ai} < v_{\rm A0} < v_{\rm Ae}$) for a magnetic twist ($B_\theta/B_z$) of 0.1.

single straight tube is much greater for longer wavelengths. For $k_z a = 0.5$ a 10% difference due to the annulus is increased to 16% by a twist, B_θ/B_z, of just 0.05 whereas a twist an order of magnitude larger, of over 0.5, is necessary for a similar increase when $k_z a = 4$. The value of P^* when there is no twist (when $B_\theta/B_z = 0$) does not change linearly with $k_z a$, instead there is a maximum value that occurs between $k_z a = 0.5$ and $k_z a = 2$ which is discussed in Carter & Erdélyi (2007) (see Sect. 2.4.1 and Fig. 6).

A similar effect is found for the other surface mode at $r = R$, with a phase speed in the vicinity of $c_{\rm ke}$, compared with a single tube with inner Alfvén speed $v_{\rm A0}$ (see Fig. 5). Here we find that single tube to straight annulus period differences of 4, 11 and 13%, for example, are increased to 7, 16 and 18% for an applied twist of 0.2 for $ka = 4$, 1 and 0.5, respectively.

3.2. Dense tubes

We now model the tube as a density enhancement with uniform longitudinal magnetic field strength throughout ($\rho_{\rm i} > \rho_0 \gg \rho_{\rm e}$, $B_{\rm i} = B_0 = B_{\rm e}$) so that $v_{\rm Ai} < v_{\rm A0} \ll v_{\rm Ae}$. Figures 6 and 7 show, for twist of 0.1 and 0.5, the dispersion curves for Eqs. (6a,b) for the $m = 1$ (kink) modes for dense tube parameters. Again, the infinite set of body modes is apparent and it broadens as twist is increased. The body/surface mode separation envelope is, as in the photospheric tube case, asymmetric and stretches to larger phase speeds as $k_z a$ decreases as do the phase speeds of the body modes. Short wavelength body modes are highly dispersive while the two surface modes are practically non-dispersive. The relative difference, P^*, between the periods, P, of the surface modes found in the twisted annulus case and the periods, $P_{\rm ER}$, of the surface mode found in the straight incompressible magnetic tube case are plotted in Figs. 8 and 9.

Figure 8 is the relative change in period for the surface mode at the inner boundary, $r = a$, (the mode at $c_{\rm ki}$ in Figs. 8 and 9) with single tube inner Alfvén speed equal to the core Alfvén speed in the annulus model and Fig. 9 is for the other surface mode at $r = R$ (with phase speed around $c_{\rm ke}$) compared to the single tube with internal Alfvén speed equal to the annulus' Alfvén speed. In both cases the addition of the uniform twist reduces the period of the mode, countering the increase in period found to occur due to the annulus region. Since the two effects on period seem to work against each other, this may be

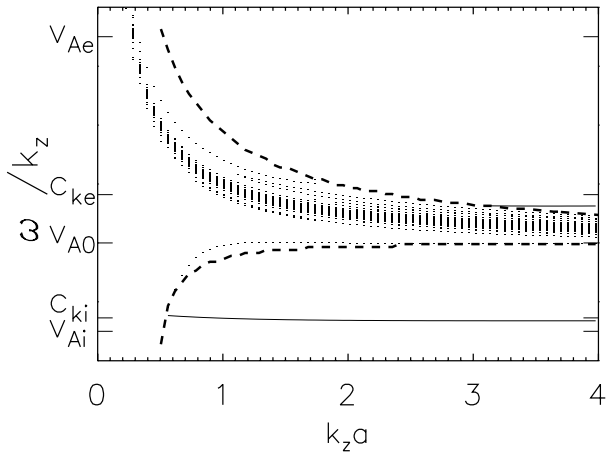

Fig. 7. Same as Fig. 6 but for a magnetic twist of 0.5.

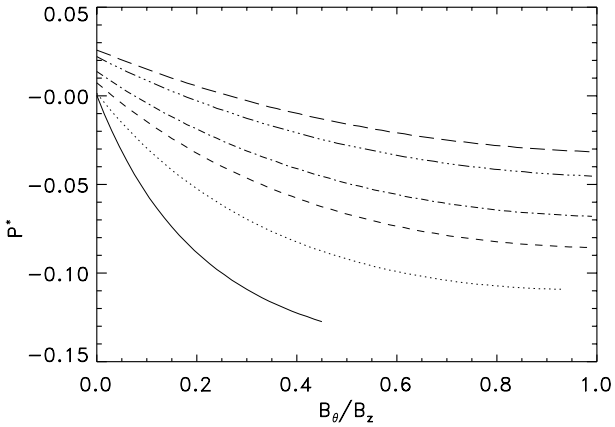

Fig. 8. Same as Fig. 4 but for parameters appropriate for a dense tube.

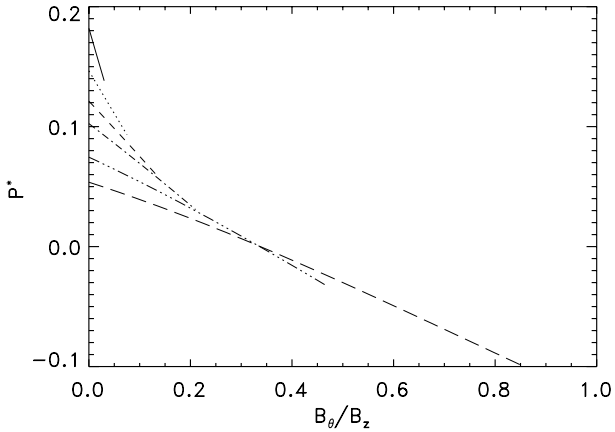

Fig. 9. Same as Fig. 5 but for parameters appropriate for a dense tube.

harder to observationally justify. By studying the intersection of the plotted lines of P^* with the y-axis (when twist = 0) in Fig. 8 we conclude that, for the straight annulus, the period of the surface mode, compared to the period of the mode for the single tube, is increased by just up to 3%. A uniform twist applied to the annulus region reduces this effect and the phase speed of the mode is reduced to up to 10% below that of the single tube.

Figure 9 shows the difference between the period, P, of the other surface mode at the external surface, $r = R$, with phase speed close to $c_{\rm ke}$ and the straight tube period, $P_{\rm ER}$. This mode, apparent from Figs. 6 and 7, does not exist for longer

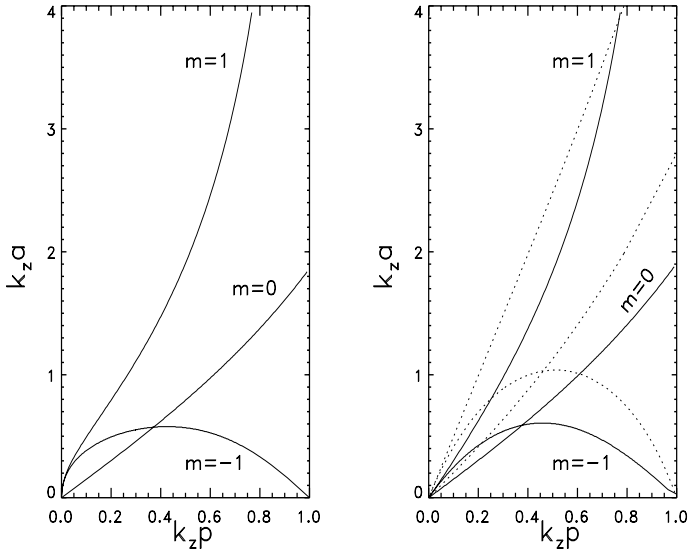

Fig. 10. Curves of marginal stability ($\omega \equiv 0$) for a single twisted tube (*left*) and for a twisted annulus configuration with a straight magnetic core with relative annulus width $a/R = 0.2$ (solid) and 0.9 (dotted).

wavelengths unless the twist is particularly small which makes the analysis on the mode less conclusive. The general trend, however, is still clear. While the annulus layer acts to increase the periods of the modes (in comparison to the single tube periods) the addition of twist counters this and for a twist, B_θ/B_z, of around 0.3 the periods are approximately equal to those of the straight tube with neither twist nor annulus.

4. Stability

It is known that the existence of twist to a flux tube gives rise to a current sheet at the boundaries which introduces a factor of instability (Dungey & Loughhead 1954; Roberts 1956) and the kink ($m = 1$) mode is the most unstable. In the analysis of this paper we assume that the applied twist is sufficiently weak that the modes studied remain stable. It is not our intention in this paper to make a rigorous analytical study of stability aspects of the current configuration. It is possible, however, by setting $\omega \equiv 0$ in the dispersion relation Eqs. (6a,b), to numerically plot the curves of marginal stability. These are shown in Fig. 10 where we plot the dimensionless wavenumber $k_z a$ as a function of dimensionless pitch $k_z p$ where $2\pi p = B_0/A_0$. Modes found to occur below these marginal stability curves are stable whilst modes above are unstable. Figure 10 shows that the addition of a straight core region to a twisted tube has a stabilising effect on the system. The left hand plot is for the case of a single twisted tube (Bennett et al. 1999) and the right hand plot shows the stability curves for the current configuration for two different relative core widths.

5. Asymptotic expansion

It is now of interest to consider the cases of large (and small) $k_z a$, $k_z R$ corresponding to the short (and long) wavelength approximations. This allows us to have a first insight into oscillations and MHD waves in a magnetically twisted core-shell problem for the kink oscillations. In addition, we investigate what happens to the solutions when the annulus has small twist and when the annulus is comparatively thin.

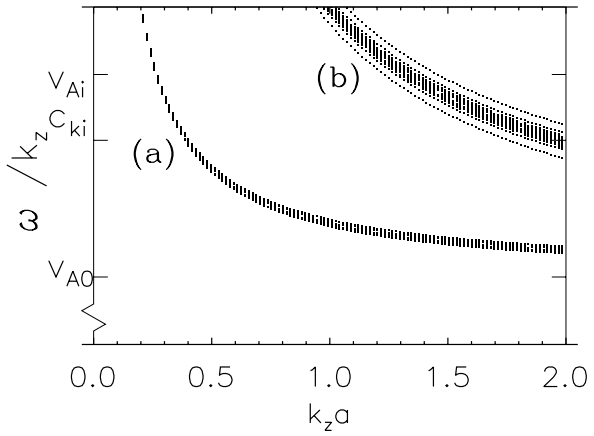

Fig. 11. Plot of the solutions to Eq. (11) of the body kink modes in the long wavelength approximation for typical photospheric parameters ($v_{\rm Ai} > v_{\rm A0} > v_{\rm Ae}$) for twists ($B_\theta/B_z$) of (a) 0.1 and (b) 0.5.

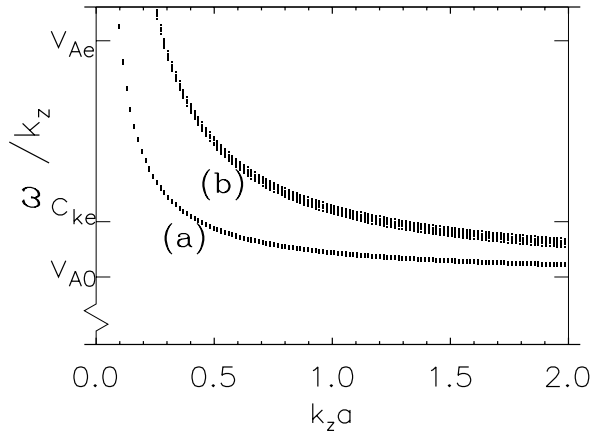

Fig. 12. Same as Fig. 11 but for parameters modelling a dense tube ($v_{\rm Ai} < v_{\rm A0} < v_{\rm Ae}$).

5.1. Long wavelength ($k_z a < k_z R \ll 1$)

First we focus on the long wavelength approximation for surface modes. It is required that

$$\frac{4c_{a\theta}^2 v_{\rm A0}^2}{(c_{\rm ph}^2 - v_{\rm A0}^2)^2} < (k_z a)^2 \tag{8}$$

to ensure $m_0^2 > 0$ (surface mode criteria). For the long wavelength approximation, the inequality $k_z a \ll 1$ implies that the LHS of Eq. (8) is also much less than 1. For this to occur for all considered magnitudes of twist (and hence for any $c_{a\theta}$) we require that $(c_{\rm ph}^2 - v_{\rm A0}^2)/v_{\rm A0}^2 \gg 1$, i.e. the phase speed is greatly different to the longitudinal component of Alfvén speed in the annulus, $v_{\rm A0}$, so that $(c_{\rm ph}/v_{\rm A0}) \gg 1$. This restriction, alongside the allowable range of phase speeds means that there are no surface modes for longer wavelengths. This is a result also seen in the single tube plots found by Bennett et al. (1999).

When studying the body modes ($-m_0^2 = n_0^2 > 0$) it is first useful to note that for $k_z a < k_z R \ll 1$ we find that

$$\frac{k_z a I_1'(k_z a)}{I_1(k_z a)} \approx 1 \tag{9}$$

and

$$\frac{k_z R K_1'(k_z a)}{K_1(k_z R)} \approx -1 \tag{10}$$

for Bessel functions I and K, and in which the dash $'$ denotes the derivative with respect to the argument. The general dispersion relation, Eq. (6b), in the long wavelength approximation then reduces to

$$\frac{(c_{\rm ph}^2 - v_{\rm A0}^2)\mathcal{Y}_a - \frac{2c_{a\theta}v_{\rm A0}}{k_z a} + 4v_{\rm A0}^2}{(c_{\rm ph}^2 - v_{\rm A0}^2)\mathcal{J}_a - \frac{2c_{a\theta}v_{\rm A0}}{k_z a} + 4v_{\rm A0}^2}\frac{Y_1(n_0 a)}{J_1(n_0 a)} = \frac{Y_1(n_0 R)}{J_1(n_0 R)}\frac{(c_{\rm ph}^2 - v_{\rm A0}^2)\mathcal{Y}_R - \frac{2c_{R\theta}v_{\rm A0}}{k_z R} + 4v_{\rm A0}^2}{(c_{\rm ph}^2 - v_{\rm A0}^2)\mathcal{J}_R - \frac{2c_{R\theta}v_{\rm A0}}{k_z R} + 4v_{\rm A0}^2} \tag{11}$$

in which $\mathcal{Y}_a = n_0 a Y_1'(n_0 a)/Y_1(n_0 a)$ and $\mathcal{J}_a = n_0 a J_1'(n_0 a)/J_1(n_0 a)$ where a is interchangeable for R, the latter corresponding to the external boundary. Solutions to this approximate dispersion relation are plotted in Figs. 11 and 12 for characteristic photospheric tube and dense tube parameters and for different values of twist. The plots clearly show that the phase speeds of the body modes for long wavelengths increase as $k_z a$ decreases and the broadening and increase in phase speeds of modes in the infinite set as twist becomes larger.

For the case of small twist ($(c_{a\theta}/v_{\rm A0}) \ll 1$) we are able to simplify Eq. (11) and reduce the approximate dispersion relation to

$$\ln(n_0 a) = (R/a)^2 \ln(n_0 R) \tag{12}$$

with solution for $c_{\rm ph}$ given by

$$c_{\rm ph}^2 = v_{\rm A0}^2 \pm \frac{2v_{\rm A0}c_{R\theta}}{\left((k_z R)^2 + (a/R)^{2a^2/(R^2-a^2)}\right)^{1/2}}. \tag{13}$$

5.2. Short wavelength, $k_z R > k_z a \gg 1$

It can be shown, see e.g. Spruit (1982) or Edwin & Roberts (1983) that, for an incompressible plasma,

$$\mathrm{div}\, \boldsymbol{v} \sim (k_z a)^m \tag{14}$$

for azimuthal wavenumber m. For the kink modes $m = 1$ and for a low-β plasma this indicates that there are no incompressible kink waves in this $k_z R > k_z a \gg 1$ limit, since otherwise the assumption of incompressibility would be satisfied rather poorly. Therefore, the analysis here is carried out for the photospheric type model only in which the short or even intermediate wavelength approximation remains still valid.

For $k_z R > k_z a \gg 1$ let us first consider the body waves. Since

$$(m_0 a)^2 = (k_z a)^2 - \frac{4c_{a\theta}^2 v_{\rm A0}^2}{(c_{\rm ph}^2 - v_{\rm A0}^2)^2} \tag{15}$$

and for body modes we require $m_0^2 < 0$, it follows that

$$\frac{4c_{a\theta}^2 v_{\rm A0}^2}{(c_{\rm ph}^2 - v_{\rm A0}^2)^2} > (k_z a)^2 \gg 1. \tag{16}$$

This inequality is satisfied for very large twist (which is unrealistic as the tube would obviously become unstable) or for $(c_{\rm ph}^2 - v_{\rm A0}^2)^2 \ll 1$ so that the phase speed, $c_{\rm ph}$, is approximately the longitudinal Alfvén speed, $v_{\rm A0}$. This is consistent with the

short wavelength tendencies in the full problem dispersion diagrams, Figs. 2 and 3.

When studying the surface modes we first notice that for the short wavelength approximation ($k_zR > k_za \gg 1$), since Eq. (15) holds, that $m_0a, m_0R \gg 1$ is also true (this is for any $c_{a\theta}$ and provided $c_{\rm ph} \not\approx v_{\rm A0}$). Expanding the Bessel functions $I_1(z)$, $I_1'(z)$, $K_1(z)$ and $K_1'(z)$ for $z \gg 1$ we are able, for $k_zR > k_za \gg 1$, to reduce the dispersion relation Eq. (6a) to

$$\frac{\rho_{\rm i}c_{\rm di}(m_0a-1)+\rho_0m_0ac_{\rm d0}+\rho_0c_{a\theta}^2(m_0a+\frac{1}{2})}{\rho_{\rm i}m_0ac_{\rm di}-\rho_0m_0ac_{\rm d0}+\rho_0c_{a\theta}^2(m_0a-\frac{1}{2})} \times {\rm e}^{2m_0(R-a)}\left(1+\frac{3(R-a)}{4m_0aR}\right) = \frac{\rho_{\rm e}m_0Rc_{\rm de}-\rho_0m_0Rc_{\rm d0}-\rho_0c_{R\theta}^2(m_0R+\frac{1}{2})}{\rho_{\rm e}c_{\rm de}(m_0R-1)+\rho_0m_0Rc_{\rm d0}-\rho_0c_{R\theta}^2(m_0R-\frac{1}{2})}, \quad (17)$$

in which $c_{\rm di} = c_{\rm ph}^2 - v_{\rm Ai}^2$, $c_{\rm d0} = c_{\rm ph}^2 - v_{\rm A0}^2$, and $c_{\rm de} = c_{\rm ph}^2 - v_{\rm Ae}^2$.

Solutions to Eq. (17) are plotted for parameters approximating a photospheric tube with different values of twist in Figs. 13. The plots indicate a relatively non-dispersive nature of the modes for large k_za which is also apparent in the full dispersion plots (Figs. 2 and 3).

In the thin annulus limit, $m_0(R-a) \ll 1$, and by noting that, for short wavelengths, m_0a and m_0R can be approximated by

$$m_0a = k_za\sqrt{1-\frac{4c_{a\theta}v_{\rm A0}}{(c_{\rm ph}^2-v_{\rm A0}^2)^2(k_zR)^2}} \approx k_za,$$

$$m_0R = k_zR\sqrt{1-\frac{4c_{R\theta}v_{\rm A0}}{(c_{\rm ph}^2-v_{\rm A0}^2)^2(k_zR)^2}} \approx k_zR,$$

it is possible to further reduce Eq. (17) to a quadratic one in $c_{\rm ph}^2$ yielding

$$c_{\rm ph}^2 = c_{k_{\rm mod}}^2 + \frac{\rho_0(c_{R\theta}^2-c_{a\theta}^2)}{\rho_{\rm i}(1-\frac{1}{2k_za})+\rho_{\rm e}(1-\frac{1}{2k_zR})} \quad (18)$$

valid as $k_za, k_zR \to \infty$, in which

$$c_{k_{\rm mod}}^2 = \frac{\rho_{\rm i}v_{\rm Ai}^2(1-\frac{1}{2k_za})+\rho_{\rm e}v_{\rm Ae}^2(1-\frac{1}{2k_zR})}{\rho_{\rm i}(1-\frac{1}{2k_za})+\rho_{\rm e}(1-\frac{1}{2k_zR})}. \quad (19)$$

6. Conclusions

In this paper we extend the study of sausage modes in a magnetic flux tube structured as a magnetically twisted annulus and straight core embedded in a straight magnetic ambient incompressible plasma (Fig. 1) investigated previously by Erdélyi & Carter (2006) to include the kink modes.

The general dispersion relation (Eqs. (6a,b)) is now studied for the $m = 1$ (i.e. kink) modes. Numerical solutions to this dispersion relation show, as in the $m = 0$ sausage mode case, an infinite set of body modes occurring due to the introduction of magnetic twist. In the sausage mode case this set is found to be symmetrical about the longitudinal component of Alfvén speed in the twisted annulus region, $v_{\rm A0}$. The set of kink body modes, however, is not symmetrical, the twist is found to increase the phase speeds of the modes proportional to $1/k_za$ so that they approach infinity at longer wavelengths. For shorter wavelengths the body modes do in fact approach $v_{\rm A0}$ from above as $c_{R\theta}/k_zR \to 0$.

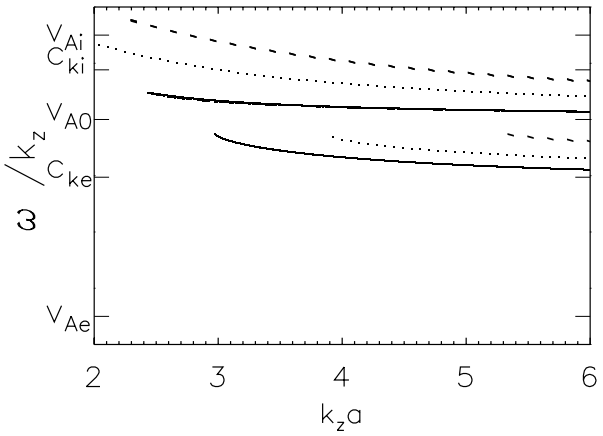

Fig. 13. Plot of solutions to Eq. (17), the short wavelength approximation for the surface kink modes, for typical photospheric parameters ($v_{\rm Ai} > v_{\rm A0} > v_{\rm Ae}$) for a twist ($B_\theta/B_z$) of 0.1 (solid), 0.3 (dotted) and 0.5 (dashed).

Two surface modes exist for the twisted shell configuration, one due to each surface (at $r = a$ and $r = R$), where one mode is trapped by the inner tube, the other by the annulus itself. Two characteristic speeds arise for this configuration, the inner surface kink speed, $c_{\rm ki}$ and the external surface kink speed, $c_{\rm ke}$ given by

$$c_{\rm ki}^2 = \frac{\rho_0v_{\rm A0}^2+\rho_{\rm i}v_{\rm Ai}^2}{\rho_0+\rho_{\rm i}}, \quad c_{\rm ke}^2 = \frac{\rho_0v_{\rm A0}^2+\rho_{\rm e}v_{\rm Ae}^2}{\rho_0+\rho_{\rm e}}. \quad (20)$$

By studying the relative (i.e. normalised) percentage change of periods compared to the single straight monolithic tube we are able to deduce more clearly the effect that the existence and magnitude of the twist has on the periods of these surface modes. For each of the two surface modes we have two natural options of normalisation. For the mode at the inner ($r = a$) surface we applied the single tube inner Alfvén speed as the core Alfvén speed, $v_{\rm Ai}$, whereas for the mode on the outer ($r = R$) surface the longitudinal component of Alfvén speed in the annulus $v_{\rm A0}$ was implemented.

For a physical condition perhaps closer to the one in the solar photosphere (when the core Alfvén speed is greater than in the annulus and external regions due to an enhancement of the magnetic field) we find that the twist strengthens the effect of the straight annulus alone (see Mikhalyaev & Solov'ev 2005; Carter & Erdélyi 2007). A straight annulus, i.e. when twist, $B_\theta/B_z = 0$, decreases the periods of the inner surface mode by between 10 and 15% (depending on the value of k_za). This decrease is extended, by a twist of less than 0.5, to between 16 and 19% (see Fig. 4). A similar result was found for the outer ($r = R$) surface mode – an initial reduction of 4–13% is increased to a reduction of 17–19% for a magnetic twist of 0.2.

For parameters approximating a dense tube (constant magnetic field strength but higher density within the tube) the effect of a twisted magnetic annulus on the oscillation periods was quite different. While the annulus layer (without twist) increased the periods of the mode, when twist was applied it acted to decrease the periods. For the surface mode at $r = a$, an initial *increase* (for an annulus with no twist) of 0–5% is reduced to a deficit by the addition of a magnetic twist: a *decrease* in period of 2–12% is seen for a twist of 0.5. The same trend arose for

the mode at the outer ($r = R$) surface with a twist of around 0.3 reducing an increase of 5–18% (with no twist) to zero, essentially negating the effect of the annulus.

This study has given a first insight into the effect of magnetic twist in an annulus region on the phase speeds and periods of propagating kink modes in a magnetically twisted shell. It is hoped that this work can provide additional information that can be used in the study of, specifically, lower atmospheric kink oscillations such as those observed recently by Kukhianidze et al. (2006); Zaqarashvili et al. (2007). Future work could include a twist in the core region, multiple shells or the extension to the fully compressible case.

Acknowledgements. The authors thank M. Ruderman and N. Venkov for a number of useful discussions. RE acknowledges M. Kéray for patient encouragement. The authors are also grateful to NSF, Hungary (OTKA, Ref. No. K67746) and to The University of Sheffield (White Rose Consortium) for the financial support they received.

References

Ashwanden, M. J. 2004, Physics of the Solar Corona (Chichester, UK: Praxis Publishing Ltd.)
Banerjee, D., Erdélyi, R., O'Shea, E., & Oliver, R. 2007, Sol. Phys., 246, 3
Bennett, K., Roberts, B., & Narain, U. 1999, Sol. Phys., 185, 41
Carter, B. K., & Erdélyi, R. 2004, in Coronal Heating, ESA SP-575, ed. R. W. Walsh, et al., 378
Carter, B. K., & Erdélyi, R. 2007, A&A, 475, 323
Dungey, J. W., & Loughhead, R. E. 1954, Austr. J. Phys., 7, 5
Edwin, P. M., & Roberts, B. 1983, Sol. Phys., 88, 179
Erdélyi, R. 2006, Phil. Trans. Royal Soc. A, 364, 351
Erdélyi, R., & Carter, B. K. 2006, A&A, 455, 361
Erdélyi, R., & Fedun, V. 2006, Sol. Phys., 238, 41
Erdélyi, R., & Fedun, V., 2007, Sol. Phys., 246, 101
Kukhianidze, V., Zaqarashvili, T. V., & Khutsishvili, E. 2006, A&A, 449, 35
Mikhalyaev, B. B., & Solov'ev, A. A. 2004, Astron. Lett., 30, 268
Mikhalyaev, B. B., & Solov'ev, A. A. 2005, Sol. Phys., 227, 249
Nakariakov, V. M., & Verwichte, E. 2005, LRSP, 2, 3
Roberts, P. H. 1956, ApJ, 124, 430
Spruit, H. C. 1982, Sol. Phys., 75, 3
Zaqarashvili, T. V., Khutsishvili, E., Kukhianidze, V., & Ramishvili, G. 2007, A&A, 474, 627